Global flash multifocal electroretinogram: Early detection of local functional changes and its correlations with optical coherence tomography and visual field tests in diabetic eyes

Lung JCY[1],

Swann PG[1, 2],

Wong DSH[3],

Chan HHL[1],

[1]Laboratory of Experimental Optometry (Neuroscience), School of Optometry, The Hong Kong Polytechnic University, Hong Kong SAR, China.

[2]School of Optometry, The Queensland University of Technology, Queensland, Australia.

[3]Eye Institute, Li Ka Shing Faculty of Medicine, The University of Hong Kong, Hong Kong SAR, China.

Author for correspondence: Dr. Henry HL Chan

Request for reprints: Dr. Henry HL Chan

Address: School of Optometry, The Hong Kong Polytechnic University, Hung Hom, Kowloon, Hong Kong SAR, China

Tel: (852) 2766-7937

Fax: (852) 2764-6051

E-mail: henryhl.chan@polyu.edu.hk

Disclaimer: Presented in part at the May 2010 ARVO meeting, Fort Lauderdale, Florida, U.S.A.

None of the authors have any proprietary interest.

Keywords and summary statement

Keywords:

1) Diabetes mellitus
2) Diabetic retinopathy
3) Multifocal Electroretinogram
4) Visual field
5) Retinal nerve fiber thickness
6) Retinal functions

Summary statement:

In this study, the correlations between the modified multifocal electroretinogram paradigm with clinical functional and morphological assessments were investigated in the human diabetic retina.

Abstract

Purpose: To investigate the correlations of the global flash multifocal electroretinogram (MOFO mfERG) with common clinical visual assessments – Humphrey perimetry and Stratus circumpapillary retinal nerve fiber layer (RNFL) thickness measurement in type II diabetic patients.

Methods: Forty-two diabetic patients participated in the study: ten were free from diabetic retinopathy (DR) while the remainder suffered from mild to moderate non-proliferative diabetic retinopathy (NPDR). Fourteen age-matched controls were recruited for comparison. MOFO mfERG measurements were made under high and low contrast conditions. Humphrey central 30-2 perimetry and Stratus OCT circumpapillary RNFL thickness measurements were also performed. Correlations between local values of implicit time and amplitude of the mfERG components (direct component (DC) and induced component (IC)), and perimetric sensitivity and RNFL thickness were evaluated by mapping the localized responses for the three subject groups.

Results: MOFO mfERG was superior to perimetry and RNFL assessments in showing differences between the diabetic groups (with and without DR) and the controls. All the MOFO mfERG amplitudes (except IC amplitude at high contrast) correlated better with perimetry findings (Pearson's r ranged from 0.23 to 0.36, $p<0.01$) than did the mfERG implicit time at both high and low contrasts across all subject groups. No consistent correlation was found between the mfERG and RNFL assessments for any group or contrast conditions.

Conclusion: The responses of the local MOFO mfERG correlated with local perimetric sensitivity but not with RNFL thickness. Early functional changes in the diabetic retina seem to occur before morphological changes in the RNFL.

Introduction

Diabetes mellitus (DM) is a group of systemic disorders resulting in hyperglycemia. Vascular anomalies are common complications of DM. The earliest visible sign of vascular anomalies in the eyes are microaneurysms, which lead to the diagnosis of diabetic retinopathy (DR) [1]. DR is one of the leading causes of blindness in the working-age population [2].

In a rat model, Barber and co-workers demonstrated that neural apoptosis occurs shortly after DM is induced [3-6]. They proposed that neural apoptosis would cause functional and anatomical changes of the inner retina even before the existence of visible vascular lesions. With the development of new diagnostic instruments, changes in the retinal nerve fiber layer (RNFL) thickness have been evaluated in diabetic patients. Optical coherence tomography (OCT) is an optical diagnostic instrument which provides an objective and non-invasive measurement of cross-sectional retinal thickness. Thinning of the neuronal layer has been reported in the human diabetic retina [7-11]. Visual function, assessed by automated perimetry, which provides a subjective measurement of luminance increment sensitivity at different visual field locations, has also been shown to be disturbed before visible DR lesions occur [10,12-15]. These two common clinical assessments have been reported to be useful in detecting early changes in diabetic retina [7-12,16].

The full-field flash electroretinogram (Flash ERG) and multifocal electroretinogram (mfERG) [17], have been reported to detect functional changes objectively in the human diabetic retina at an early stage [18-31]. In our previous study [32], a modified global flash mfERG (MOFO mfERG) paradigm was applied to examine early functional changes in the diabetic retina. The MOFO mfERG helps in separating the

"middle" and "inner" retinal responses. There are two main components in the MOFO mfERG response: the direct component (DC) (predominantly from the middle retina) and the induced component (IC) (predominantly from the inner retina) [33]. It has been found that both the middle and inner retinal functions deteriorate before the vascular lesions are visible in DM patients [32].

In the present study, we aim to compare the findings of our electrophysiological assessment with the automated perimetry and the OCT RNFL thickness measurements in the diabetic retina, in order to understand their relationships at the early stages of DM and to study the difference of the correlations between tests at various levels of DR severity.

Methods

Subjects

Forty-two patients with type II DM were recruited for the study: ten (aged 51.0 ± 6.9 years) were free from DR while thirty-two (aged 49.5 ± 5.8 years) had non-proliferative diabetic retinopathy (NPDR). Fourteen healthy controls (aged 49.4 ± 7.0 years) were recruited for comparison. All subjects had visual acuity better than 6/9. Their refractive errors were between +3.00 D and -6.00 D and astigmatism was less than -1.25 D. Subjects with systemic or ocular diseases other than DM or DR were excluded. Detailed eye examination including dilated fundus examination was carried out for each subject. One eye was randomly selected for this study.

The instantaneous plasma glucose data were obtained from ten controls and forty diabetic patients using a plasma-glucose meter (Accu-Chek Compact Plus, F.

Hoffmann-La Roche Ltd, Basel, Switzerland); testing occurred more than two hours after any food intake.

All procedures of the study followed the tenets of the Declaration of Hesinki. This study was approved by the Ethics Committee of The Hong Kong Polytechnic University. Informed consent was obtained from each subject following full explanation of the experimental procedures.

Measurement

1) mfERG stimulation and recording

A VERIS Science 5.1 system (Electro-Diagnostic-Imaging, Redwood City, CA, USA) was used for the MOFO mfERG measurement. The instrumental set-up was similar to that described in our previous studies [32,34,35]. Briefly, the mfERG stimulation was a 103 scaled hexagonal pattern which subtended 47° horizontally and 44° vertically. It was displayed on a high luminance CRT monitor (FIMI Medical Electrical Equipment, MD0709BRM, Saronno, Italy) with a frame rate of 75 Hz. A cycle of the MOFO mfERG stimulation included four video frames: a multifocal flash frame, a dark frame, a global flash frame and another dark frame. The multifocal frames were modulated between bright and dark phases according to a binary pseudo-random m-sequence (2^{13}-1). Each subject had the mfERG measurement made at both high contrast (98% contrast; bright phase: 200 cd/m^2; dark phase: 2 cd/m^2) and low contrast (46% contrast; bright phase: 166 cd/m^2; dark phase: 61 cd/m^2) in random order with the background luminance of 100 cd/m^2. The measurement for each contrast level was divided into 32 segments and lasted for about 8 minutes. Short breaks were provided between segments. Any segment with blinks or eye movements was discarded and re-recorded immediately.

One eye of each subject, with the pupil dilated by 1% tropicamide (Alcon, Fort Worth, TX, USA), was randomly selected for mfERG measurement. A Dawson-Trick-Litzkow (DTL) electrode was used as the active electrode. A gold-cup reference electrode was placed 10 mm lateral to the outer canthus of the tested eye, and a similar ground electrode was placed on the central forehead. The signal was amplified 100,000 times with the bandpass from 3 to 300 Hz (Grass Instrument Co., Quincy, MA, USA). The amplitudes and implicit times of the DC and IC for both contrast conditions (Fig. 1) were measured as described in previous studies [32,34-37].

2) Optic coherence tomography (OCT)

The circumpapillary retinal nerve fiber layer (RNFL) thickness was measured using the Stratus OCT (Carl Zeiss Meditec, Inc., Dublin, CA, USA) using the fast scanning mode. The scanning area was circular with a 3.4 mm diameter. The circle centre was aligned with the centre of the optic nerve head. The RNFL thickness within the circular region was further divided into 12 sectors and the sectoral RNFL thickness was then used for analysis (see below).

3) Visual field (VF)

The Humphrey Field Analyzer (Carl Zeiss Meditec, Inc., Dublin, CA, USA) was used to measure monocular visual field in this study. The white-on-white static protocol "Central 30-2 (SITA-fast)" was chosen to assess the central 60 degree field; full-aperture lenses were placed in front of the patient's tested eye to correct refractive errors for the viewing distance of the VF analyzer. The locations of the VF test spots were plotted on a grid; the grid was then overlaid with the mfERG topography which was divided into 35 regions for further analysis [18,35,38,39]. The overlay is shown as in fig. 2. Details of the grid scaling and alignment are discussed below.

4) Fundus photodocumentation

A Topcon IMAGEnet fundus camera was used to take fundus photographs of the tested eye centrally and at eight peripheral locations for each subject. The photographs were then combined to form a mosaic for each subject.

Data analysis

1) MOFO mfERG parameters

The 103 mfERG trace arrays were divided into 35 regions as suggested by Bearse and co-workers [18,39]. The mfERG from left eyes was reflected so that all data resembled those from right eyes. The amplitudes and implicit times of the local MOFO mfERG responses (i.e. DC and IC) were collected for analysis (Fig. 1). For each region, data of mfERG parameters from the control group were used to calculate the means and standard deviations (SD) which were then used to calculate z-scores of the mfERG parameters. Using z-scores for further analysis helps in eliminating topographic asymmetry of the mfERG and provides the same basis for comparison [18,35,39-41]. Each subject had 35 regional z-scores (calculated based on the regional means and SD of the control group) across one's own mfERG topography. An averaged z-score could thus be obtained across the 35 regions for individual subject.

2) Visual field (VF) sensitivity

In the Humphrey visual field analyzer, two parameters could be obtained directly from the print-out: mean deviation (MD) and local total deviation (TD). MD is the numerical value of averaged VF sensitivity difference from the age-norm provided by the manufacturer of Humphrey analyzer. TD is the numerical value which indicates the difference from the age-norm at each tested location on the field. In this study, the MD

and local TD were used for analysis in order to provide the same basis for comparison among different subject groups [42,43]. The MD was correlated with the plasma glucose level to evaluate the relationship in between and compared among the three subject groups. The TD of each VF test spot which fell in the mfERG topography was used to map with the mfERG responses in order to evaluate its correlation with the electrophysiological assessment.

3) RNFL thickness

The mean RNFL thickness and the RNFL thickness values obtained in each of the 12 sectors measured by the OCT within the circular scanning region were used for analysis. The averaged RNFL thickness of each subject correlated with the plasma glucose level and compared among the three subject groups. To eliminate topographic asymmetry, the sectoral RNFL thicknesses of the control group were used to calculate the sectoral z-scores for individual subject as suggested by Bronson-Castain and co-workers [19]. At each sector of RNFL thickness, the values from the control group were firstly averaged. This value was then used to calculate the sectoral z-score of each subject using: [(Individual sectoral thickness – averaged sectoral thickness from controls)/ averaged sectoral thickness from controls]. This provides the same basis for comparison among the three groups of regional data after mapping between mfERG topography and RNFL profile.

4) Duration of DM, plasma glucose level and averaged findings of the three ocular assessments (mfERG, RNFL thickness and VF sensitivity)

Duration of DM among the diabetic patients was ranked in 3 categories: less than 5 years, duration ranged from 5 to 10 years, duration more than 10 years. Median of the duration ranking was reported for the diabetic groups in the results below.

Plasma glucose level and the averaged results of the three ocular assessments were compared among the control subjects, the DM patients without DR and the DM patients with NPDR using one-way ANOVA; significance levels were adjusted using Bonferroni's correction. Pearson's correlation (r) was evaluated between the plasma glucose level and the averaged mfERG responses, mean RNFL thickness and VF MD among the three subject groups.

5) Correlations of the local retinal responses among three ocular assessments by mapping

Fundus photographs, mfERG data and VF data were all provided at different scales. They were converted to a common scale by measuring the distance from fovea/ fixation point to disc centre/ blindspot depression. This was used as a baseline to adjust the scale of the two-dimensional data.

a) Mapping of the fundus photographs with the mfERG topography

As mentioned above, a mosaic photograph was formed for each individual. By overlapping the fovea and optic disc of the photographs with the central peak and blindspot depression of the mfERG topography respectively, the mosaic photographs were aligned with the 103-hexagonal mfERG topography. Fundus photographs were then divided into 35 regions following the mfERG topography in fig. 2 [18,39]. A retinal specialist who was masked to each patient's diagnosis then rated each region for presence or absence of a DR lesion.

This was done for the three groups of subjects, thus allowing creation of three groups of regional data:

Group I – Regional data from the control group only

Group II – Regional data from the DM patients (without any DR signs) only

Group III – Regional data from the DM patients with NPDR only, but only those with DR lesions were included. Those regions without DR lesions were discarded to avoid confusion with group II

b) Mapping of the mfERG topography with the VF test grid

The 103 hexagonal stimulus pattern of mfERG was aligned with the VF test grid. The locations of the blindspot and the fixation point (i.e. foveal peak) in mfERG topography were overlaid with the blindspot and fixation point of the VF test grid respectively. By overlaying the VF test grid with the 35-division mfERG topography as shown in fig. 2, the mfERG parameters measured at each division could be grouped with the TD of the VF test spot that fell within the division. If more than one VF test spot fell within the same mfERG division, the TD of those VF test spots were averaged before matching with the mfERG parameters. As the Humphrey central 30-2 program (central 60°) provides a larger field of view than that of mfERG (~ 47°), those VF test spots which fell outside the mfERG topography were excluded from the study. Once groupings of mfERG parameters and VF TD values were accomplished, correlation values were calculated.

c) Mapping of the mfERG topography with the OCT RNFL thickness profile

The OCT RNFL profile at the optic disc was mapped with the VF test grid (Fig. 2) according to the overlay generated by Garway-Heath and co-workers [44,45]. The fundus locations mapped by Garway-Heath et al. are on a 3° grid, making alignment of their data and ours a simple matter. Together with the mapping applied in the above section between the mfERG topography and the VF test grid, we were able to link the MOFO mfERG topography to its corresponding sectoral RNFL profile obtained from

the OCT measurement (Fig. 2). If more than one mfERG division fell along a sector of the RNFL profile, the z-scores of the mfERG parameters at that sector were averaged before mapping with the RNFL thickness. The correlation between the regional MOFO mfERG responses and the sectoral RNFL thickness could then be studied.

d) The correlations (Pearson's r) between the local z-scores of the MOFO mfERG responses and the results of two clinical assessments (VF and OCT) were calculated for group I (regional data from the control group), II (regional data from the DM patients without any DR signs) and III (regional data from the DM patients with NPDR).
The regional responses of the three ocular assessments (mfERG, RNFL thickness and VF sensitivity) were also compared among group I, II and II. Due to the repeated contribution from individual subject, generalized estimating equation (GEE) with Bonferroni's post-hoc adjustment was used for statistical analysis with the assumption of unstructured working matrix.

Results

Correlations of the local mfERG responses with the local sensitivity deviation (TD) of VF

After overlaying the MOFO mfERG topography with VF test spots, there were 76 VF test spots which fell into the mfERG topography. This gave a total of 854 VF regional data points: 392 in group I, 280 in group II and 182 in group III (Table 1). The correlations of the local mfERG responses with the local VF TD are shown in table 2 for different groups of data (Group I, II and III). The mfERG amplitude provides a more consistent relationship with the VF findings across various groups than implicit time does.

1) MOFO mfERG amplitude z-scores

At both high and low contrast levels, the DC and IC amplitudes showed a positive correlation with VF local sensitivity deviation in all three groups of data (except the IC amplitude of group II at high contrast level). Retinal regions with higher luminance sensitivity also showed greater mfERG amplitudes. The Pearson's correlation value ranged from 0.24 to 0.42 ($p<0.05$) (Table 2) (Fig. 3-4). However, the variations of the correlation did not show any trend in terms of the DR lesions or contrast levels.

2) MOFO mfERG implicit time z-scores

No significant correlations with visual field results were found in the diabetic groups (group II and III) in terms of the DC implicit time at either contrast level. For the IC implicit time, significant correlations were found in group II but not in group III at high and low contrast levels. However, the relationship between the IC implicit time and luminance sensitivity was inconsistent across the diabetic groups.

Correlations of the local MOFO mfERG responses with the sectoral RNFL thickness z-scores

There were 398 sectoral RNFL thickness z-scores after mapping with the mfERG topography: 168 in group I, 120 in group II and 110 in group III (Table 1). However, no significant differences were found among these three groups of data ($p>0.05$).

The correlations between the mfERG responses with the sectoral RNFL thickness are listed in (Table 3). No significant trends found in correlations between MOFO mfERG parameters and sectoral RNFL thickness; few statistical significant correlations were found between in terms of IC amplitude z-score. However, these correlations were not consistent with the changes of contrast levels or among the various subject groups.

Regional data of Group I, II and III from each measurement (MOFO mfERG, VF and RNFL) after mapping based on mfERG topography

For the MOFO mfERG, there were a total of 1074 regional data values: 490 in group I, 350 in group II and 234 in group III (Table 1).

Only the amplitudes of the DC at low contrast level and IC at the high contrast level were able to differentiate the diabetic data (group II and III) from the control data (group I) ($p<0.05$). The amplitudes from the diabetic groups were significantly smaller than those of the control group. There was a significant delay in high contrast DC and IC for group III ($p<0.05$), compared to group I data ($p<0.05$). There was a further delay of DC response in group III in high contrast condition than group II ($p<0.05$). DC and IC implicit time findings did not differentiate between diabetic data (group II and III) and the control data.

Compared with the corresponding VF regional data points after overlaying the MOFO mfERG topography with VF test spots as shown in table 1, it was found that only the regions with DR lesions demonstrated a marked reduction in VF sensitivity ($p<0.01$) compared to the regional data from the controls (group I).

However, for the sectoral RNFL thickness z-scores collected after mapping with the MOFO mfERG topography (Table 1), no significant differences were found among these three groups of data ($p>0.05$).

Relationship of the plasma glucose levels with the averaged mfERG responses, VF sensitivity deviation and RNFL thickness

The control subjects had significantly lower plasma glucose levels than did the diabetic patients, either with or without DR ($p<0.02$ and $p<0.01$ respectively) (Table 4).

The MOFO mfERG IC amplitude z-score for the low contrast condition in the control group increased with the plasma glucose level ($r=0.731$, $p<0.02$). There were no significant correlations between DC or IC amplitude z-scores at either contrast level and glucose level for either group of diabetic patients. No significant correlations were found between plasma glucose levels and RNFL thickness or VF assessments in all groups of subjects (controls, DM patients with or without DR).

Discussion

Our findings demonstrated that the MOFO mfERG responses generally correlated better with the results of perimetric testing than those of the RNFL thickness measurement in diabetes. Among these three assessments, only the MOFO mfERG differentiates the "No DR" regional data (group II) from the control group (group I). The MOFO mfERG amplitude provides a more consistent relationship with the clinical perimetric test across retinal regions than does implicit time. RNFL thickness has no relationship with the functional testing performed in this study.

We found that the local VF sensitivity deviation (i.e. TD), rather than the RNFL thickness, was moderately correlated with most of the MOFO mfERG parameters in the control data. It is not surprising that an electrophysiological assessment correlates better with a clinical functional test than with a morphological test in these subjects. Visual field assessment has been applied in studies of DM patients, but whether VF measures can differentiate diabetic patients without DR from healthy controls is still

controversial. It is generally accepted that the VF mean deviation should decrease with increasing DR severity [10,12,16,46,47].

Two main components are found in the global flash stimulation of the mfERG: the direct component (DC) and induced component (IC) [37]. Pharmacological dissection of the responses in the porcine eye indicates that the DC component mainly originates from the bipolar cells with some oscillatory responses from the inner retina and there is little contribution from the photoreceptors. The IC component mainly originates from the inner retina, especially the ganglion cells [33]. Under the stimulation with less than 60% contrast, the inner retinal response becomes more obvious [48-50]. This paradigm has been applied in various ocular diseases to study changes in retinal adaptation [25,36,51-53].

Correlations between mfERG amplitudes and VF parameters were more consistent than correlations between implicit time and VF parameters in the diabetic samples (group II and III). Only group II showed a significant negative association between the VF and the IC implicit time. There was an opposite change in the correlation direction from group I to group II (as shown in table 2) for the high and low contrast conditions. Although the mechanisms for the mfERG amplitude and implicit time changes in DM patients are not understood, neither reduced contrast levels nor the increased DR severity led to a great change in the values of Pearson's r between MOFO mfERG parameters and VF sensitivity deviations. This result should be repeated to determine whether the relationship between VF and IC implicit time can be substantiated or whether it is anomalous. In both previous [25,32,35] and current studies, the amplitudes of the MOFO mfERG paradigm demonstrated a greater ability in showing the group difference between the healthy and diabetic groups (with or without DR); moreover, it

also showed a better and more consistent correlation with the perimetric functional test than the implicit time. These findings are different to those reported in other mfERG paradigm studies [20,54-57] that delay of implicit time existed earlier before the amplitude changes in DM patients. This discrepancy between the amplitude and implicit time findings would be probably due to the different mfERG paradigms involved in the studies which may in turn trigger a different cellular performance.

Similar to a previous study [38], Pearson's correlation r between the mfERG and VF was maintained at about 0.2 to 0.4. The relatively weak to moderate correlations between these two functional tests may be due to different underlying mechanisms. MOFO mfERG provides an objective measurement of the retinal adaptation activity predominantly from retinal components beyond the secondary neural level, while VF provides a subjective measurement of the retinal threshold detection from the whole visual system. Although the MOFO mfERG was shown to be better than VF in differentiating DM patients without DR from the control group, it cannot be concluded that mfERG is superior to VF. One of the major differences between VF and mfERG is that VF provides a static stimulus for assessing luminance sensitivity while mfERG measures activities to luminance changes and temporal interactions. The information from these two tests is supplementary and gives rise to a clearer picture of the underlying changes in DM. The functional deterioration in the diabetic retina found in this study cannot be purely explained by the luminance detection/ sensitivity or the morphological changes of the RNFL. The changes observed in MOFO mfERG and its weak to moderate correlations with RNFL thickness and luminance sensitivity indicated the alteration of adaptive function in the middle and/or inner retinal layers (with the RNFL excluded).

While there are some conservative opinions on the ability of OCT to detect RNFL thinning for the DM patients without visible DR lesions [9,11], many studies have proposed that there is RNFL thinning, at least in a specific quadrant of the optic disc, in the early stages of NPDR [7-9,11,58]. In the present study, functional deterioration was found but no structural anomalies were detected in early DM. Only the IC amplitude findings provided a weak correlation with RNFL morphological changes. Zhang and co-workers [59] suggested that retrograde axonal transport was impaired in the early stage of DM. The ganglion cells would be adversely affected before morphological impairment of the optic nerve fibers. This may indicate why the retinal functional deterioration found by the MOFO mfERG paradigm in DM patients does not match with RNFL changes, and the optic neuropathy found in DM patients is very different from the glaucomatous optic neuropathy [8,9]. This weak electrophysiological-morphological association further supports the hypothesis raised by Greenstein et al. [60] that the problematic site of DM is at/near the middle retinal layers which is different from glaucoma or retinitis pigmentosa (RP).

Hyperglycemia is an underlying problem in DM. Unexpectedly, the high correlation of the plasma glucose level to the IC amplitude in the low contrast condition was shown only in the healthy controls but not in the diabetic patients. This might be due to the different effects caused by glycemic control and chronic hyperglycemia [10,61,62]. Further studies on how glycemic control and chronic hyperglycemia affect middle/inner retinal responses (as reflected in mfERG responses) in both normal and diabetic patients would be useful. Another limitation of this study is the mapping between the RNFL bundles with the OCT which was based on a Caucasian population. Whether there is any ethnic difference in the mapping of the RNFL to each OCT sector needs to be investigated.

Conclusion

MOFO mfERG results correlated better with the results of the VF test than with the morphological findings from the OCT test in diabetic patients. Impairment of retinal adaptation can be identified in the early stages of diabetes using the MOFO mfERG. The perimetric-electrophysiological association is not strengthened by the existence of NPDR.

Impairment of short-term retinal adaptation in early diabetic patients is not related to any reduction of RNFL thickness. Further studies with better plasma glucose control and measurement should be carried out to investigate the effect of chronic and transient hyperglycemia on the visual system. The functional changes in the middle and inner retinal layers in the early stages of DM before appearance of visible lesions may be a potential target in planning the future treatment of the diabetic retina.

Acknowledgement:

This study was supported by the Associated Fund (Research Postgraduate) from The Hong Kong Polytechnic University, Internal Research Grants (GU585, GU858) and the Niche Areas –Myopia Research (J-BB7P) and Glaucoma Research (J-BB76) from The Hong Kong Polytechnic University. Special thanks to Prof. Brian Brown for his valued assistance.

Reference

1. Van Bijsterveld OP (2000) Diabetic retinopathy. Martin Dunitz Ltd, London:2

2. Porta M, Bandello F (2002) Diabetic retinopathy - A clinical update. Diabetologia 45 (12):1617-1634

3. Barber AJ (2003) A new view of diabetic retinopathy: a neurodegenerative disease of the eye. Prog Neuropsychopharmacol Biol Psychiatry 27 (2):283-290

4. Barber AJ, Gardner TW, Abcouwer SF (2011) The significance of vascular and neural apoptosis to the pathology of diabetic retinopathy. Invest Ophthalmol Vis Sci 52 (2):1156-1163

5. Barber AJ, Lieth E, Khin SA, Antonetti DA, Buchanan AG, Gardner TW (1998) Neural apoptosis in the retina during experimental and human diabetes. Early onset and effect of insulin. J Clin Invest 102 (4):783-791
6. Kern TS, Barber AJ (2008) Retinal ganglion cells in diabetes. J Physiol 586 (Pt 18):4401-4408
7. Lopes de Faria JM, Russ H, Costa VP (2002) Retinal nerve fibre layer loss in patients with type 1 diabetes mellitus without retinopathy. Br J Ophthalmol 86 (7):725-728
8. Oshitari T, Hanawa K, Adachi-Usami E (2009) Changes of macular and RNFL thicknesses measured by Stratus OCT in patients with early stage diabetes. Eye (Lond) 23 (4):884-889
9. Ozdek S, Lonneville YH, Onol M, Yetkin I, Hasanreisoglu BB (2002) Assessment of nerve fiber layer in diabetic patients with scanning laser polarimetry. Eye (Lond) 16 (6):761-765
10. Parravano M, Oddone F, Mineo D, Centofanti M, Borboni P, Lauro R, Tanga L, Manni G (2008) The role of Humphrey Matrix testing in the early diagnosis of retinopathy in type 1 diabetes. Br J Ophthalmol 92 (12):1656-1660
11. Takahashi H, Chihara E (2008) Impact of diabetic retinopathy on quantitative retinal nerve fiber layer measurement and glaucoma screening. Invest Ophthalmol Vis Sci 49 (2):687-692
12. Bengtsson B, Heijl A, Agardh E (2005) Visual fields correlate better than visual acuity to severity of diabetic retinopathy. Diabetologia 48 (12):2494-2500
13. Bresnick GH, Condit RS, Palta M, Korth K, Groo A, Syrjala S (1985) Association of hue discrimination loss and diabetic retinopathy. Arch Ophthalmol 103 (9):1317-1324
14. Ismail GM, Whitaker D (1998) Early detection of changes in visual function in diabetes mellitus. Ophthalmic Physiol Opt 18 (1):3-12
15. Kurtenbach A, Flogel W, Erb C (2002) Anomaloscope matches in patients with diabetes mellitus. Graefes Arch Clin Exp Ophthalmol 240 (2):79-84
16. Bengtsson B, Hellgren KJ, Agardh E (2008) Test-retest variability for standard automated perimetry and short-wavelength automated perimetry in diabetic patients. Acta Ophthalmol 86 (2):170-176
17. Sutter EE, Tran D (1992) The field topography of ERG components in man--I. The photopic luminance response. Vision Res 32 (3):433-446
18. Bearse MA Jr, Han Y, Schneck ME, Barez S, Jacobsen C, Adams AJ (2004) Local multifocal oscillatory potential abnormalities in diabetes and early diabetic retinopathy. Invest Ophthalmol Vis Sci 45 (9):3259-3265
19. Bronson-Castain KW, Bearse MA Jr, Neuville J, Jonasdottir S, King-Hooper B, Barez S, Schneck ME, Adams AJ (2009) Adolescents with type 2 diabetes early

indications of focal retinal neuropathy, retinal thinning, and venular dilation. Retina 29 (5):618-626
20. Fortune B, Schneck ME, Adams AJ (1999) Multifocal electroretinogram delays reveal local retinal dysfunction in early diabetic retinopathy. Invest Ophthalmol Vis Sci 40 (11):2638-2651
21. Holopigian K, Greenstein VC, Seiple W, Hood DC, Carr RE (1997) Evidence for photoreceptor changes in patients with diabetic retinopathy. Invest Ophthalmol Vis Sci 38 (11):2355-2365
22. Kizawa J, Machida S, Kobayashi T, Gotoh Y, Kurosaka D (2006) Changes of oscillatory potentials and photopic negative response in patients with early diabetic retinopathy. Jpn J Ophthalmol 50 (4):367-373
23. Luu CD, Szental JA, Lee SY, Lavanya R, Wong TY (2010) Correlation between retinal oscillatory potentials and retinal vascular caliber in type 2 diabetes. Invest Ophthalmol Vis Sci 51 (1):482-486
24. Palmowski AM, Sutter EE, Bearse MA Jr, Fung W (1997) Mapping of retinal function in diabetic retinopathy using the multifocal electroretinogram. Invest Ophthalmol Vis Sci 38 (12):2586-2596
25. Shimada Y, Li Y, Bearse MA Jr, Sutter EE, Fung W (2001) Assessment of early retinal changes in diabetes using a new multifocal ERG protocol. Br J Ophthalmol 85 (4):414-419
26. Yamamoto S, Kamiyama M, Nitta K, Yamada T, Hayasaka S (1996) Selective reduction of the S cone electroretinogram in diabetes. Br J Ophthalmol 80 (11):973-975
27. Chen H, Zhang M, Huang S, Wu D (2008) The photopic negative response of flash ERG in nonproliferative diabetic retinopathy. Doc Ophthalmol 117 (2):129-135
28. Schneck ME, Bearse MA Jr, Han Y, Barez S, Jacobsen C, Adams AJ (2004) Comparison of mfERG waveform components and implicit time measurement techniques for detecting functional change in early diabetic eye disease. Doc Ophthalmol 108 (3):223-230
29. Tyrberg M, Ponjavic V, Lovestam-Adrian M (2005) Multifocal electroretinography (mfERG) in insulin dependent diabetics with and without clinically apparent retinopathy. Doc Ophthalmol 110 (2-3):137-143
30. Xu J, Hu G, Huang T, Huang H, Chen B (2006) Using multifocal ERG responses to discriminate diabetic retinopathy. Doc Ophthalmol 112 (3):201-207
31. Yamamoto S, Takeuchi S, Kamiyama M (1997) The short wavelength-sensitive cone electroretinogram in diabetes: relationship to systemic factors. Doc Ophthalmol 94 (3):193-200
32. Lung JCY, Tang GYB, Chu PHW, Ng YF, Chan HHL (2009) Abstracts of the XLVII International Symposium of the ISCEV (International Society for Clinical

Electrophysiology of Vision). Global flash mfERG in the early detection of the local functional chnages of diabetic retinopathy lesions. Doc Ophthalmol 119 Suppl 1:17-92
33. Chu PH, Chan HH, Ng YF, Brown B, Siu AW, Beale BA, Gilger BC, Wong F (2008) Porcine global flash multifocal electroretinogram: possible mechanisms for the glaucomatous changes in contrast response function. Vision Res 48 (16):1726-1734
34. Lung JC, Chan HH (2010) Effects of luminance combinations on the characteristics of the global flash multifocal electroretinogram (mfERG). Graefes Arch Clin Exp Ophthalmol 248 (8):1117-1125
35. Lung JC, Swann PG, Chan HH (2012) Early local functional changes in the human diabetic retina: a global flash multifocal electroretinogram study. Graefes Arch Clin Exp Ophthalmol. E-pub ahead. [PMID: 22527315]
36. Chu PH, Chan HH, Brown B (2006) Glaucoma detection is facilitated by luminance modulation of the global flash multifocal electroretinogram. Invest Ophthalmol Vis Sci 47 (3):929-937
37. Shimada Y, Bearse MA Jr, Sutter EE (2005) Multifocal electroretinograms combined with periodic flashes: direct responses and induced components. Graefes Arch Clin Exp Ophthalmol 243 (2):132-141
38. Han Y, Adams AJ, Bearse MA Jr, Schneck ME (2004) Multifocal electroretinogram and short-wavelength automated perimetry measures in diabetic eyes with little or no retinopathy. Arch Ophthalmol 122 (12):1809-1815
39. Bearse MA Jr, Han Y, Schneck M, Adams A (2003) Enhancement and mapping of inner retinal contributions to the human multifocal electroretinogram (mfERG). Invest Ophthalmol Vis Sci 44:ARVO E-abstract 2696
40. Sutter EE, Bearse MA Jr (1999) The optic nerve head component of the human ERG. Vision Res 39 (3):419-436
41. Wu S, Sutter EE (1995) A topographic study of oscillatory potentials in man. Vis Neurosci 12 (6):1013-1025
42. Dersu I, Wiggins MN (2006) Understanding visual fields, Part II; Humphrey visual fields. Journal of Ophthalmic Medical Technology 2 (3)
43. Heijl A, Patella VM (2002) Essential perimetry: The field analyzer primer. 3rd edn. Carl Zeiss Meditec AG, Germany
44. Garway-Heath DF, Holder GE, Fitzke FW, Hitchings RA (2002) Relationship between electrophysiological, psychophysical, and anatomical measurements in glaucoma. Invest Ophthalmol Vis Sci 43 (7):2213-2220
45. Garway-Heath DF, Poinoosawmy D, Fitzke FW, Hitchings RA (2000) Mapping the visual field to the optic disc in normal tension glaucoma eyes. Ophthalmology 107 (10):1809-1815

46. Nitta K, Saito Y, Kobayashi A, Sugiyama K (2006) Influence of clinical factors on blue-on-yellow perimetry for diabetic patients without retinopathy: comparison with white-on-white perimetry. Retina 26 (7):797-802
47. Remky A, Weber A, Hendricks S, Lichtenberg K, Arend O (2003) Short-wavelength automated perimetry in patients with diabetes mellitus without macular edema. Graefes Arch Clin Exp Ophthalmol 241 (6):468-471
48. Bearse MA Jr, Sutter EE (1999) Contrast dependence of multifocal ERG components. Vision Science and Its Applications, OSA Technical Digest Series 1:24-27
49. Hood DC, Greenstein V, Frishman L, Holopigian K, Viswanathan S, Seiple W, Ahmed J, Robson JG (1999) Identifying inner retinal contributions to the human multifocal ERG. Vision Res 39 (13):2285-2291
50. Sutter EE, Shimada Y, Li Y, Bearse MA Jr (1999) Mapping inner retinal function through enhancement of adaptation components in the M-ERG. Vision Science and Its Applications, OSA Technical Digest Series 1:52-55
51. Feigl B, Brown B, Lovie-Kitchin J, Swann P (2005) Adaptation responses in early age-related maculopathy. Invest Ophthalmol Vis Sci 46 (12):4722-4727
52. Luo X, Patel NB, Harwerth RS, Frishman LJ (2011) Loss of the low-frequency component of the global-flash multifocal electroretinogram in primate eyes with experimental glaucoma. Invest Ophthalmol Vis Sci 52 (6):3792-3804
53. Palmowski-Wolfe AM, Todorova MG, Orguel S, Flammer J, Brigell M (2007) The 'two global flash' mfERG in high and normal tension primary open-angle glaucoma. Doc Ophthalmol 114 (1):9-19
54. Bearse MA Jr, Adams AJ, Han Y, Schneck ME, Ng J, Bronson-Castain K, Barez S (2006) A multifocal electroretinogram model predicting the development of diabetic retinopathy. Prog Retin Eye Res 25 (5):425-448
55. Han Y, Bearse MA Jr, Schneck ME, Barez S, Jacobsen CH, Adams AJ (2004) Multifocal electroretinogram delays predict sites of subsequent diabetic retinopathy. Invest Ophthalmol Vis Sci 45 (3):948-954
56. Harrison WW, Bearse MA Jr, Ng JS, Jewell NP, Barez S, Burger D, Schneck ME, Adams AJ (2011) Multifocal electroretinograms predict onset of diabetic retinopathy in adult patients with diabetes. Invest Ophthalmol Vis Sci 52 (2):772-777
57. Ng JS, Bearse MA Jr, Schneck ME, Barez S, Adams AJ (2008) Local diabetic retinopathy prediction by multifocal ERG delays over 3 years. Invest Ophthalmol Vis Sci 49 (4):1622-1628
58. Sugimoto M, Sasoh M, Ido M, Wakitani Y, Takahashi C, Uji Y (2005) Detection of early diabetic change with optical coherence tomography in type 2 diabetes mellitus patients without retinopathy. Ophthalmologica 219 (6):379-385

59. Zhang L, Ino-ue M, Dong K, Yamamoto M (2000) Retrograde axonal transport impairment of large- and medium-sized retinal ganglion cells in diabetic rat. Curr Eye Res 20 (2):131-136
60. Greenstein VC, Hood DC, Ritch R, Steinberger D, Carr RE (1989) S (blue) cone pathway vulnerability in retinitis pigmentosa, diabetes and glaucoma. Invest Ophthalmol Vis Sci 30 (8):1732-1737
61. Jeppesen P, Knudsen ST, Poulsen PL, Mogensen CE, Schmitz O, Bek T (2007) Response of retinal arteriole diameter to increased blood pressure during acute hyperglycaemia. Acta Ophthalmol Scand 85 (3):280-286
62. Klemp K, Larsen M, Sander B, Vaag A, Brockhoff PB, Lund-Andersen H (2004) Effect of short-term hyperglycemia on multifocal electroretinogram in diabetic patients without retinopathy. Invest Ophthalmol Vis Sci 45 (10):3812-3819

Captions

Table 1 Regional data from each measurement according to its mapping with the MOFO mfERG topography

(*: Significantly different from the control group (Group I) with $p< 0.05$)

(†: Significantly different from the DM patients without DR (Group II) with $p<0.05$)

Table 2 Summary of Pearson's correlation (r) between local responses of VF (TD) and MOFO mfERG parameters

(*: Significantly different from the control group (Group I) with $p < 0.05$)

Table 3 Summary of Pearson's correlation (r) between local responses of RNFL sectoral z-score and MOFO mfERG parameters

(*: Significantly different from the control group (Group I) with $p < 0.05$)

Table 4 Summary of the averaged plasma glucose level (mmol/L), the median of the DM duration period (Ranking: 0 = less than 5yrs, 1 = 5 to 10yrs, 2= more than 10yrs), the VF mean deviation (dB), the RNFL thickness (um) and the averaged MOFO mfERG parameters (z-scores)

(*: Significantly different from the control group (Group I) with $p < 0.05$)

Fig. 1 MOFO mfERG resultant waveforms. The measurement of amplitudes and implicit times of DC and IC are also shown.

Fig. 2 Mapping between the data of the mfERG, VF test and OCT RNFL profile. Left side: Mapping of the overlays between the mfERG topography and the VF test spots. Right side: The sectoral RNFL profile measured by the OCT. Colour indication: Through mapping the VF test spots with the corresponding sectoral RNFL thickness according to the studies by Garway-Heath et al. [44,45], the regional mfERG data could be matched with the corresponding RNFL thickness (the central red cross represents the fixation point of the mfERG and VF assessments)

Fig. 3 Correlation between the local responses of the VF (TD) and DCA_z of the MOFO mfERG at 98% and 46% contrast conditions for Groups I, II and III

Fig. 4 Correlation between the local responses of the VF (TD) and ICA_z of the MOFO mfERG at 98% and 46% contrast conditions for Groups I, II and III

Tables

Table 1. Regional data from each measurement according to its mapping with the MOFO mfERG topography

	Group I	Group II	Group III
Visual field (VF)	(n= 392)	(n= 280)	(n= 182)
Total deviation (TD)	-1.51 ± 1.55	-1.84 ± 2.06	-3.30 ± 2.39 (* p=0.005)
OCT	(n= 168)	(n= 120)	(n= 110)
Sectoral RNFL thickness (z-score)	0.00 ± 0.97	0.02 ± 1.25	0.029 ± 1.21
MOFO mfERG	(n= 490)	(n= 350)	(n= 234)
98% contrast level (z-scores)			
DCIT _z	0.00 ± 0.96	0.02 ± 1.50	1.23 ± 1.66 (* p<0.001) († p=0.013)
DCA_z	0.00 ± 0.96	-0.67 ± 1.01	-0.62 ± 1.09
ICIT_z	0.00 ± 0.96	0.06 ± 1.68	0.75 ± 2.31 (* p=0.013)
ICA_z	0.00 ± 0.96 († p=0.045)	-0.64 ± 0.85 (* p=0.045)	-0.80 ± 0.92 (* p=0.007)
46% contrast level (z-scores)			
DCIT_z	0.00 ± 0.96	-0.15 ± 1.85	-0.02 ± 2.22
DCA_z	0.00 ± 0.96 († p=0.014)	-0.66 ± 0.90 (* p=0.014)	-0.93 ± 1.20 (* p=0.003)
ICIT_z	0.00 ± 0.96	0.20 ± 1.08	0.12 ± 1.39
ICA_z	0.00 ± 0.96	-0.12 ± 0.85	-0.47 ± 0.89

(*: Significantly different from the control group (Group I) with p< 0.05)

(†: Significantly different from the DM patients without DR (Group II) with p<0.05)

Table 2. Summary of Pearson's correlation (r) between local responses of VF (TD) and MOFO mfERG parameters

Contrast conditions	MOFO mfERG parameters	Control Samples (Group I)		No DR Samples (Group II)		DR Samples (Group III)	
		Pearson r	p-value	Pearson r	p-value	Pearson r	p-value
98%	DCIT_z	0.26	<0.001*	-0.10	0.109	-0.05	0.532
	DCA_z	0.36	<0.001*	0.28	<0.001*	0.32	<0.001*
	ICIT_z	0.22	<0.001*	-0.20	0.001*	0.03	0.719
	ICA_z	0.24	<0.001*	0.01	0.909	0.42	<0.001*
46%	DCIT_z	0.18	<0.001*	0.09	0.142	0.02	0.794
	DCA_z	0.25	<0.001*	0.24	<0.001*	0.23	<0.001*
	ICIT_z	0.16	0.002*	-0.22	<0.001*	0.06	0.427
	ICA_z	0.30	<0.001*	0.23	<0.001*	0.27	<0.001*

(*: Significantly different from the control group (Group I) with p< 0.05)

Table 3. Summary of Pearson's correlation (r) between local responses of RNFL sectoral z-score and MOFO mfERG parameters

Contrast conditions	MOFO mfERG parameters	Control Samples (Group I)		No DR Samples (Group II)		DR Samples (Group III)	
		Pearson r	p-value	Pearson r	p-value	Pearson r	p-value
98%	DCIT_z	-0.08	0.309	-0.09	0.330	0.18	0.067
	DCA_z	0.02	0.799	0.13	0.159	0.03	0.770
	ICIT_z	-0.05	0.520	-0.06	0.492	0.04	0.718
	ICA_z	-0.06	0.437	0.00	0.995	0.27	0.005*
46%	DCIT_z	-0.08	0.331	0.07	0.432	0.14	0.139
	DCA_z	-0.14	0.081	-0.00	0.968	-0.08	0.392
	ICIT_z	0.09	0.233	-0.05	0.596	-0.00	0.966
	ICA_z	-0.20	0.008*	-0.06	0.491	-0.15	0.128

(*: Significantly different from the control group (Group I) with $p < 0.05$)

Table 4. Summary of the averaged plasma glucose level (mmol/L), the median of the DM duration period, the VF mean deviation (dB), the RNFL thickness (um) and the averaged MOFO mfERG parameters (z-scores)

	Control	DM patients without DR	DM patients with NPDR
	(n= 10persons)	(n= 10persons)	(n= 30persons)
Plasma glucose level (mmol/L) (Mean ± SD)	6.59 ± 1.58	11.42 ± 4.14 (* p=0.008)	10.15 ± 3.55 (* p=0.018)
	(n = 14persons)	(n = 10persons)	(n = 32persons)
Median of the rank of DM duration	------	2.0 (6.9 ± 6.9years)	1.0 (4.6 ± 3.7years)
VF mean deviation (dB)	-1.46 ± 1.15	-2.01 ± 1.97	-3.15 ± 2.02 (* p=0.017)
RNFL average thickness (um)	(n = 14persons)	(n = 10persons)	(n = 32persons)
	114.01 ± 8.94	114.91 ± 12.34	113.26 ± 10.98
MOFO mfERG	(n= 14persons)	(n = 10persons)	(n = 32persons)
98% Contrast level (z-scores)			
DCIT_z	0.00 ± 0.70	0.02 ± 1.09	0.42 ± 1.39
DCA_z	0.00 ± 0.72	-0.67 ± 0.78	-0.59 ± 0.83
ICIT_z	0.00 ± 0.69	0.06 ± 0.94	0.21 ± 1.15
ICA_z	0.00 ± 0.74	-0.64 ± 0.60	-0.62 ± 0.66 (* p=0.018)
46% Contrast level (z-scores)			
DCIT_z	0.00 ± 0.55	-0.15 ± 0.72	0.05 ± 0.94
DCA_z	0.00 ± 0.71	-0.66 ± 0.49	-0.64 ± 0.69 (* p=0.013)
ICIT_z	0.00 ± 0.61	0.20 ± 0.57	-0.01 ± 0.68
ICA_z	0.00 ± 0.78	-0.12 ± 0.39	-0.38 ± 0.48

(*: Significantly different from the control group (Group I) with $p < 0.05$)

Fig. 1 MOFO mfERG resultant waveforms. The measurement of amplitudes and implicit times of DC and IC are also shown.

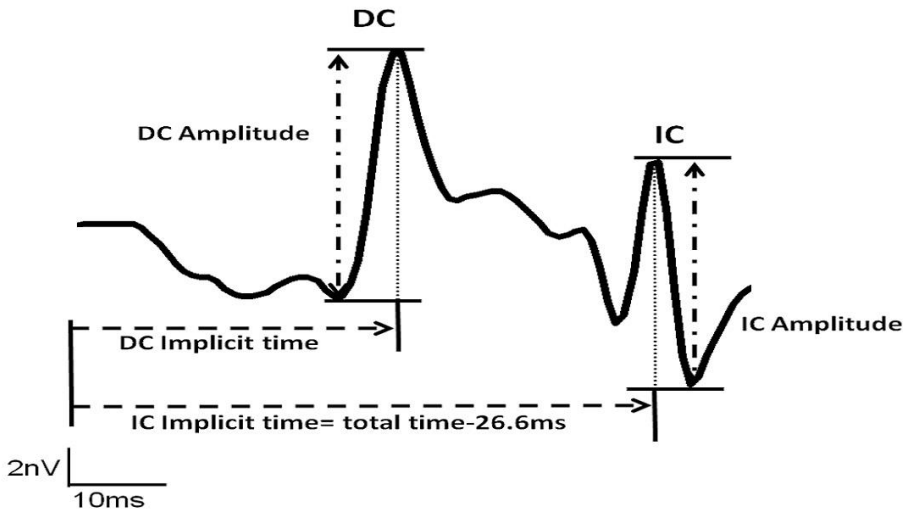

Fig. 2 Mapping between the data of the mfERG, VF test and OCT RNFL profile. Left side: Mapping of the overlays between the mfERG topography and the VF test spots.

Right side: The sectoral RNFL profile measured by the OCT. Colour indication: Through mapping the VF test spots with the corresponding sectoral RNFL thickness according to the studies by Garway-Heath et al. [44,45], the regional mfERG data could be matched with the corresponding RNFL thickness (the central red cross represents the fixation point of the mfERG and VF assessments)

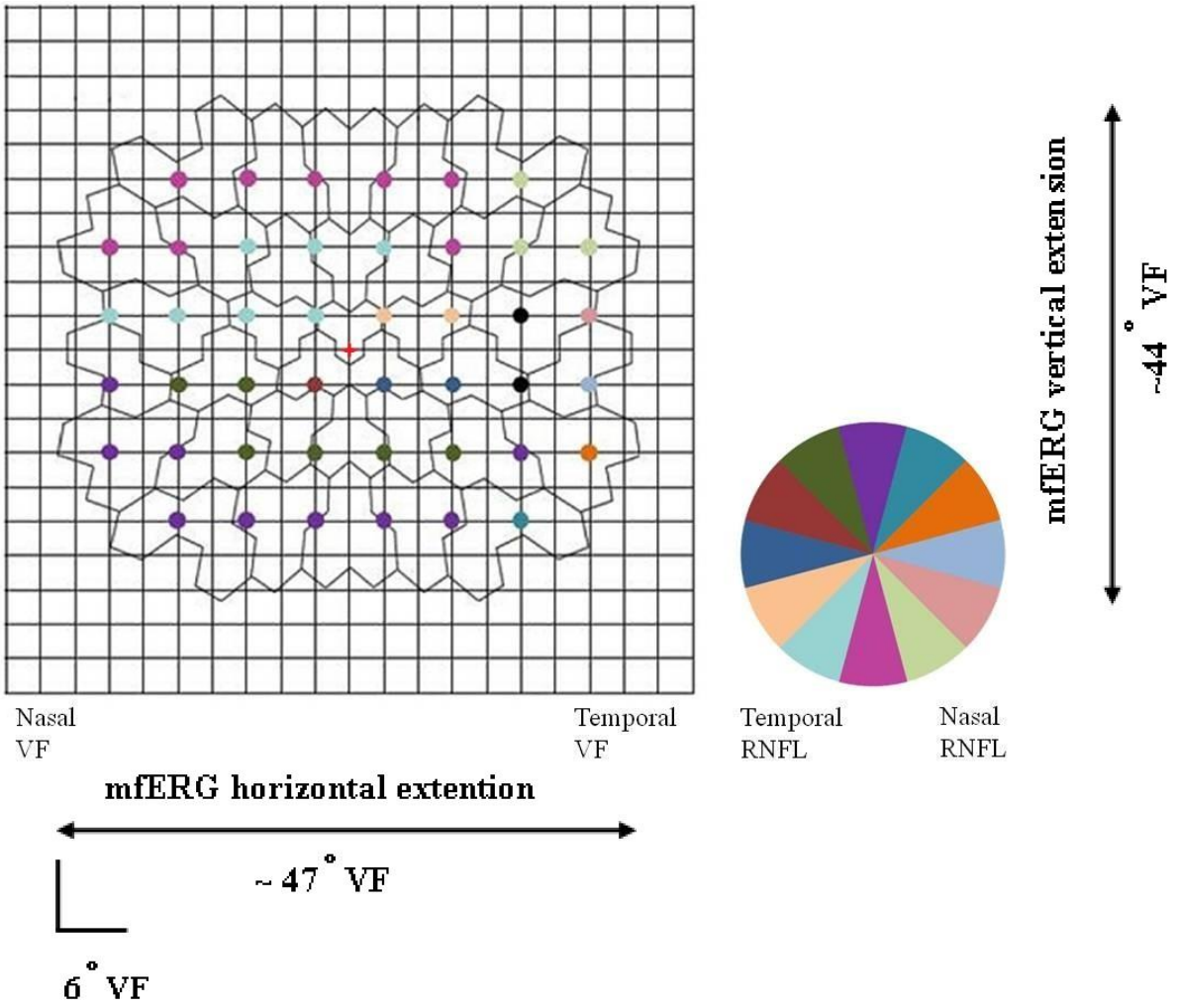

Fig. 3 Correlation between the local responses of the VF (TD) and DCA_z of the MOFO mfERG at 98% and 46% contrast conditions for Groups I, II and III

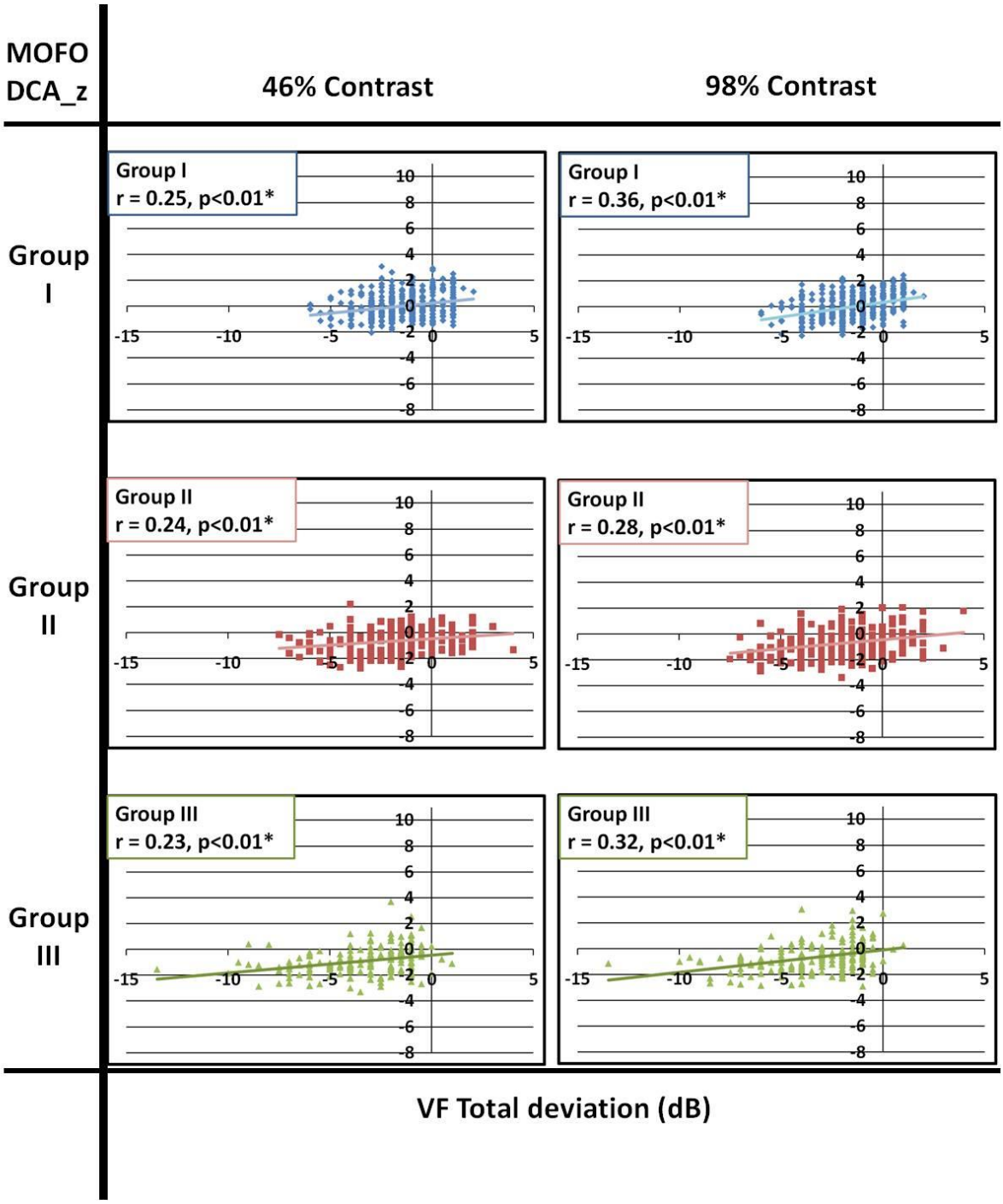

Fig. 4 Correlation between the local responses of the VF (TD) and ICA_z of the MOFO mfERG at 98% and 46% contrast conditions for Groups I, II and III